Current Applied Physics 20 (2020) 122–131

Contents lists available at ScienceDirect

Current Applied Physics

journal homepage: www.elsevier.com/locate/cap

Effects of novel benzotriazole based zwitterionic salt as electrolyte additive for lithium ion batteries

Isheunesu Phiri[a], Chris Yeajoon Bon[a], Sangjun Kim[a], Manasi Mwemezi[a], Louis Hamenu[b], Alfred Madzvamuse[c], Sang Hern Kim[a,**], Jang Myoun Ko[a,*]

[a] Department of Applied Chemistry & Biotechnology, Hanbat National University, 125 Dongseo-daero, Deokmyeong-dong, Yuseong-gu, Daejeon, South Korea
[b] Department of Chemistry School of Physical and Mathematical Sciences, College of Basic and Applied Sciences University of Ghana, Legon, Ghana
[c] Department of Chemistry, University of Zimbabwe, PO MP167, Mount Pleasant, Harare, Zimbabwe

ARTICLE INFO

Keywords:
Zwitterion
Ionic conductivity
Benzotriazole
Sulfobetaine
Solid electrolyte interface

ABSTRACT

A novel zwitterionic lithium-benzotriazole sulfobetaine is fabricated by grafting 1,3– propanesultone onto benzotriazole and then lithiating it. The resultant lithium-benzotriazole-sulfobetaine additive is used as an electrolyte additive in lithium ion batteries in 1 M $LiPF_6$ (ethylene carbonate/dimethyl carbonate = 1:1). The electrolytes with the lithium-benzotriazole sulfobetaine shows higher ionic conductivities (2.18×10^{-2} S cm^{-1}) compared to the bare electrolyte (1.07×10^{-2} S cm^{-1}) and greater electrochemical stability (anodic limit at ~5.5 V vs. Li/Li$^+$) than the pure electrolyte (anodic limit at ~4.6 V vs. Li/Li$^+$). The discharge capacity of the lithium cobalt oxide/graphite cells is improved at higher C-rates with the addition of lithium-benzotriazole sulfobetaine due to increased ionic conductivity. The lithium cobalt oxide/graphite cells with the lithium-benzotriazole sulfobetaine additive also show stable cycling performance. These findings warrant the use of lithium-benzotriazole sulfobetaine as an electrolyte additive in lithium ion batteries.

1. Introduction

Due to the surge of electronic devices and a growing interest in electric drones, electric vehicles etc., the demand for secondary lithium-ion batteries (LIBs) has also increased greatly over the last two decades and continues to rise due to their high energy density, low self-discharge rate and high open-circuit [1–4]. The LIBs are mainly composed of an electrolyte, two electrodes (cathode and anode), current collectors and a separator. Different electrolytes are used depending on the type of battery. Electrolytes can either be liquid, gel or solid [5–7]. Liquid electrolytes have high ionic conductivity and high lithium transference number but their performance is limited at very high and very low temperatures which has led to the use of various additives. The liquid electrolytes are mostly made up of a lithium salt (e.g., $LiPF_6$, LiTFSI, etc.) dissolved in organic solvents (e.g., ethylene carbonate (EC), dimethyl carbonate (DMC), propylene carbonate) [1]. The mostly used salt is $LiPF_6$ because of its high ionic conductivity and electrochemical stability [8,9]. However, the salt performance is hampered at high temperatures due to the generation of HF and PF_5 in the presence of very small amounts of moisture [4,10–12]. Myriads of salt options have been proposed instead of $LiPF_6$ [10,13,14] but some of these options either have low ionic conductivities [10,15,16] or are corrosive towards aluminum as is the case with LiTFSI or LiFSI [10] which hinders their use commercially. To improve on ionic conductivity, zwitterions have been used as additives mostly for gel and solid polymer electrolytes [17,18]. Zwitterions are molecules with both positive and negative charges in an intramolecular form [2,19,20] resulting in a large dipole moment. Because of the large dipole moment, zwitterions help in the dissociation of lithium salts thus improving the electrochemical properties of SPEs, [15,21,22]. Furthermore, it has been shown that some zwitterions are capable of dissolving inorganic salts and dissociate them into ions [23,24]. Since zwitterions have a zero net charge, they do not have ion–pair migration even under a potential, as a result they have been used to improve target–ion transportation as reported by Ohno et al. [25–27]. As a matter of fact, zwitterions have a very low ionic conductivity > 10^{-6} S cm^{-1} even at 200 °C [23] because there is no free movement of ions since they are covalently tethered. This means zwitterions do not provide carrier ions irrespective of offering an increased ion density and an inimitable atmosphere for target–ion transportation [17]. The commonly used zwitterionic electrolyte additives contain the sulfonate group (SO_3^-) which has been reported as good exchange sites for Li$^+$ ions because of the easiness to associate and

* Corresponding author.,
** Corresponding author.
E-mail addresses: shkim@hanbat.ac.kr (S.H. Kim), jmko@hanbat.ac.kr (J.M. Ko).

https://doi.org/10.1016/j.cap.2019.10.017
Received 14 August 2019; Received in revised form 8 October 2019; Accepted 17 October 2019
Available online 20 October 2019

dissociate between the SO_3^- group and Li^+ ions [21,28–32]. Moreover, zwitterions have been shown to increase rate capability, are non-volatile, enable suppression dendrite formation at low cycling rates and reduce the resistance of the solid electrolyte interphase (SEI) due to a large electrochemical window and very low volatility [21,22].

Aromatic compounds have also been used as electrolyte additives for lithium-ion batteries [24,33]. A heterocyclic compound benzotriazole (BT) has been used as an antifreeze, flame retardant and for corrosion-inhibition [35,36] and recently as an electrolyte additive [37], while succinonitrile has been used as an additive in polymer electrolyte systems [38]. These bases have high polarity that enable the dissolution of salts in electrolytes thereby improving ionic conductivities and transference numbers. Apart from their high polarity, these bases also add to thermal stability of the salts [37]. Sylvia et al. used benzimidazole (BI) in its lithium salt form as an additive. The BI binds to PF_5 in the electrolyte thereby reducing decomposition of $LiPF_6$ [34]. Hamenu et al. used BT as an electrolyte additive for a $LiPF_6$ salt electrolyte. The BT containing showed good cycling performance and better discharge capacities at high C-rates and formation of a good SEI compare to the pristine electrolyte [37]. In this study, we synthesized a benzotriazole-based zwitterionic lithium salt by grafting propanesultone in a quaternization reaction. The sulfonate group of the zwitterion has high affinity towards the Li^+ ions due to greater dipole moment of the zwitterion compared to the basic nitrogen atoms on the bare benzotriazole resulting in greater dissociation of the $LiPF_6$ in the electrolyte. The free nitrogen atom in the benzotriazole-based zwitterion also acts as a Lewis-base by donating a lone electron pair to the phosphorus atom in PF_5 form a stable complex thereby stabilizing the electrolyte. The novel zwitterionic salts showed high ionic conductivities and improved electrochemical performances compared to the pristine electrolyte and the BT containing electrolyte.

2. Experimental

2.1. Synthesis of zwitterion benzotriazole-sulfobetaine (BTSB)

Zwitterion benzotriazole-sulfobetaine (BTSB) was synthesized by a quaternization reaction of benzotriazole (Sigma-Aldrich, ReagentPlus®, 99%) with 1,3-propanesultone (98%, Sigma Aldrich) as shown in Scheme 1(a). 1,3-propanesultone (1.22 g, 0.01 mol) was added to benzotriazole (1.19 g, 0.01 mol) in anhydrous acetone (≥99.5%, Sigma Aldrich) (25 mL) under nitrogen. The reaction mixture was stirred vigorously under nitrogen for 48 h at 60 °C. The white precipitate was filtered off and repeatedly washed with anhydrous acetone. The white solid product was dried at 70 °C under vacuum for 24 h and stored under argon.

2.2. Lithiation of zwitterion benzotriazole-sulfobetaine (BTSB)

In a 100 mL flask, 0.4 g of $LiPF_6$ (> 97.0% (T), TCI chemicals) (0.0026 mol) was dissolved in 40 mL of anhydrous acetone (solubility of $LiPF_6$ in acetone is 1 g:100 g). BTSB (0.6 g) was added into the solution and ultra-sonicated for 15 min before reaction with stirring at 700 rpm at room temperature for 48 h. The product, lithium benzotriazole-sulfobetaine (Li-BTSB) was collected by vacuum filtration and washed with copious amounts of anhydrous acetone. The Li-BTSB was dried under vacuum at 60 °C overnight and stored under argon. The summary of the processes is shown in Scheme 1.

2.3. Characterization of lithium benzotriazole-sulfobetaine (Li-BTSB)

Chemical analyses of the Li-BTSB was conducted using Fourier transform infrared spectroscopy (FT-IR, Nicolet iS5, USA) and X-ray photoelectron spectroscopy (XPS) (VersaProbe II Scanning XPS Microprobe, Physical Electronics), and the thermal stability of the synthesized particles was analyzed using a thermogravimetric analyzer (TGA, N1000, SCINCO).

2.4. Electrolyte preparation and electrochemical characterization

Five electrolyte solutions were prepared. The electrolyte denoted as "pure electrolyte" is 1 M $LiPF_6$ dissolved in EC/DMC (1:1 V/V) (PanaX eTec) and the other four were made by adding 0.1 wt% and 0.5 wt% of BT and Li-BTSB and stirred for 24 h and then denoted as "0.1 wt% BT", "0.5 wt% BT", "0.1 wt% Li-BTSB" and "0.5 wt% Li-BTSB". Ionic conductivity tests for the prepared electrolytes were done using two stainless steel (1 × 0.5 cm) electrodes in an glass cuvette (Aldrich, pathlength = 10 mm). Linear sweep voltammetry (LSV) was conducted on coin-type (2032) half-cells. The half-cells were composed of stainless steel plates as working electrodes, lithium metal foil as counter and reference electrodes, liquid electrolytes with and without additives, and a polyethylene (PE) separator on an Autolab instrument (ECO CHEMIE PGSTAT 100) in a potential window of 2–7 V at a scan rate of 1 mVs^{-1}. Cyclic voltammetry (CV) measurements were carried out in the potential range of 0–3 V and a scan rate of 0.5 $mV\,s^{-1}$, with lithium foils as the reference and counter electrodes and graphite as the working electrode.

2.5. Cell preparation and electrochemical characterization

Coin-type (2032) full cells (LCO‖electrolyte‖graphite) were fabricated in an argon-filled glove box to investigate the effect of the additives on the performance of LIBs at room temperature. The anode and cathode electrodes were composed of lithium cobalt oxide (LCO, Kokam Co.) and graphite (Kokam Co.) (80 wt%) as active materials, respectively, 10 wt% Super P (Imerys, Switzerland) as a conductive additive, and 10 wt% polyvinylidene fluoride (Kreha, Japan, $M_w \approx 350{,}000$) as a polymeric binder in *N*-methyl-2-pyrrolidone (NMP, Sigma Aldrich) as a dispersing agent. To prepare the electrodes, an 8.0 w/v% solution of PVDF binder in N-methyl-2-pyrrolidone (NMP) was prepared and stirred for about 6 h. Then, a calculated volume of this solution was added to an 80:10 ratio mixture of the active materials ($LiCoO_2$ or graphite) and Super P, into a 100 mL sealed plastic cup and ball milled (1000 rpm using zirconium balls, 5 mm diameter) to a fine slurry. The viscous slurry was cast onto an aluminum foil (15 μm, Aluminum, Korea) for the LCO and copper foil (15 μm, Iljin materials) using a doctor blade apparatus. The NMP was evaporated at 80 °C for 2 h and the electrodes were further dried at 120 °C for 24 h. The electrodes were then pressed with a roll pressing machine (WV-60, Samyang 60, Korea). The electrodes were punched into spherical discs with a diameter of 14 mm and 16 mm for the cathode and anode, respectively and then further dried in a vacuum oven at 60 °C for 48 h before use thereafter they were transferred to an argon-filled glove box. The thickness of the electrodes were 39 μm and 32 μm for the cathode and anode, respectively, and the loadings of the electroactive materials were calculated to be 20.33 ± 0.5 mg and 41.82 ± 0.5 mg for LCO and graphite, respectively. Coin cells were prepared by sandwiching a PE separator (18 mm, 20 μm, Celgard) between the fabricated cathode and anode, and filling the cell with the prepared electrolyte in an argon-filled glove box. The prepared cells were aged for 12 h and then charged and discharged at constant current (CC) mode at 0.1 C in a voltage range of 2.8–4.4 V using a battery cycler (Toscot 3000, Toyo, systems) for cell formation. Subsequently, the cells were charged at 0.1 C at constant current/constant voltage (CC/CV) mode and then discharged at 0.1, 0.2, 0.5, 1, 2, 5 and 10C within the same voltage range. As a reference, the C-rate was calculated using 140 $mAh.g^{-1}$ as the experimental specific capacity of LCO. Cycling was performed by charging-discharging at 1 C. Complex impedance spectroscopy tests were carried out using an Autolab (ECO CHEMIE PGSTAT 100) in a frequency range of 10^{-2}–10^{-5} Hz after the initial and 100th cycle. The surface image of the cathode and anode electrodes was observed after the initial discharge using FE-SEM, which was equipped with an energy dispersive X-ray spectroscope to

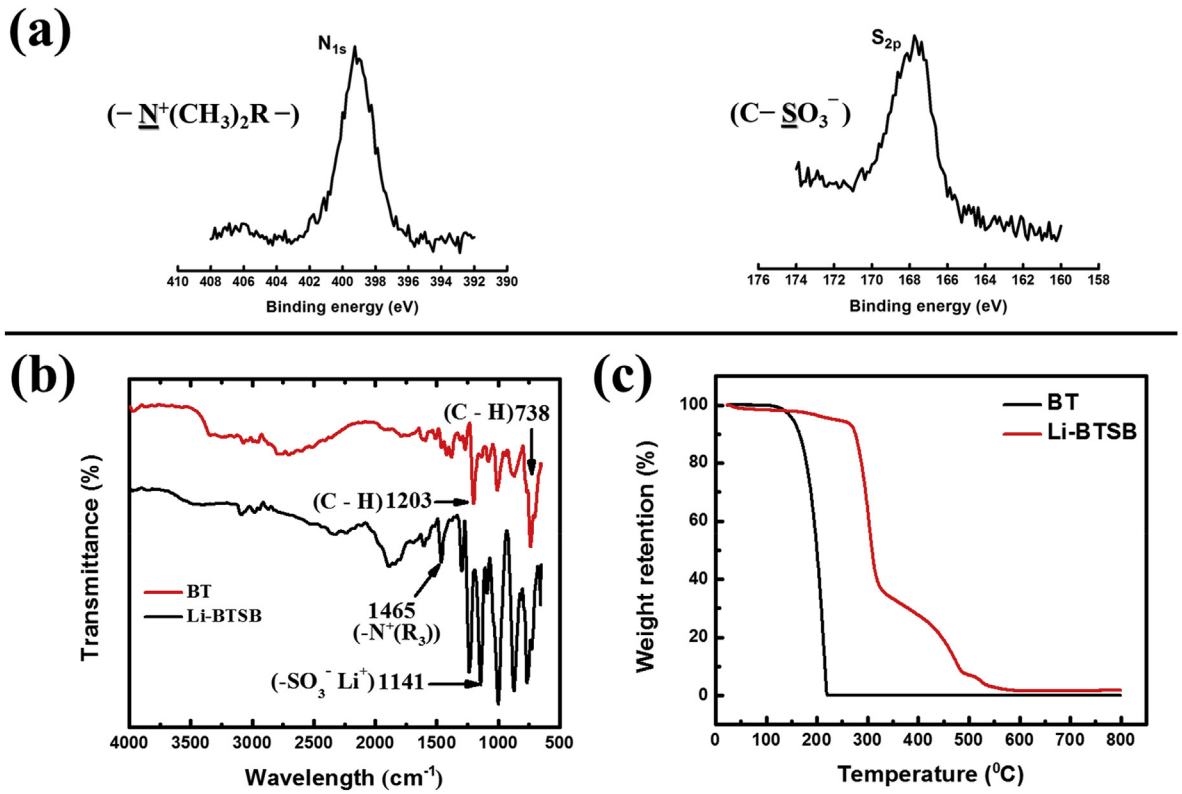

Fig. 1. Characterization of BT and Li-BTSB: (a) XPS analysis, (b) FT-IR analysis, and (c) TGA analysis.

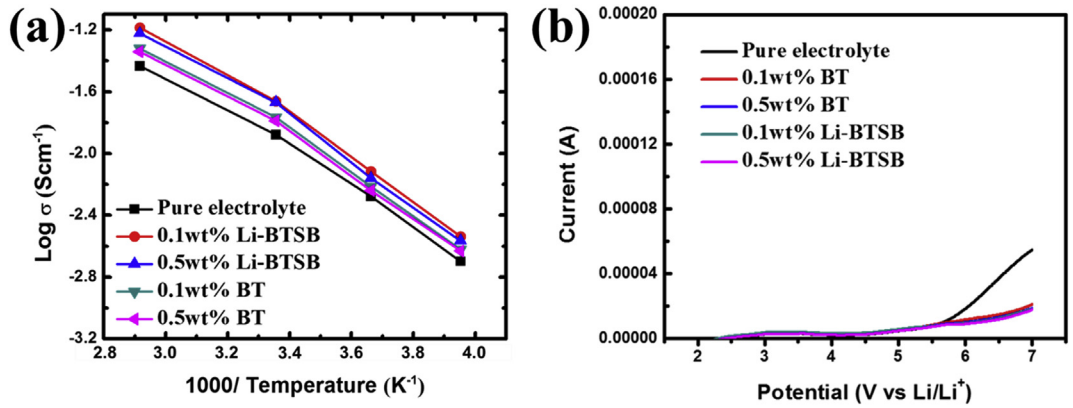

Fig. 2. (a) Arrhenius plots of the ionic conductivities and (b) Linear sweep voltammograms of the electrolytes.

Table 1
Summary of the ionic conductivities of the electrolytes.

	Ionic conductivity (mS/cm)			
	at 70°C	at 25°C	at 0°C	at −20°C
Pure electrolyte	36.86	13.16	5.25	0.53
0.1 wt% Li-BTSB	61.07	21.81	6.38	0.87
0.5 wt% Li-BTSB	59.89	21.39	6.31	0.86
0.1 wt% BT	47.88	17.10	5.87	0.68
0.5 wt% BT	45.56	16.27	5.76	0.65

determine the chemical composition of the SEI.

3. Results and discussion

3.1. Synthesis of lithium benzotriazole-sulfobetaine

Fig. 1(a) shows the XPS analysis of Li-BTSB which shows peaks at BEs of 167.8 and 168.1 eV that are attributed to the spin−orbit split doublet peak for sulphur S_{2p} in the sulfonate $C-SO_3^-$ species in the zwitterionic moiety. The peak at BE of 400.5 eV is attributed to the N1s core-level spectra peak of the quaternary ammonium cations ($-N^+(CH_3)_2R\ -$) [39–41]. The IR spectra of BT and Li-BTSB are shown in Fig. 1(b). In the spectrum of BT, bands are observed at 1203 and 738 cm^{-1}, corresponding to the C – H in-plane bending and C – H out-of-plane bending vibrations of the benzotriazole benzene ring. At 1087 cm^{-1}, there is a stretch of the benzene and triazole rings, corresponding also to N – H stretching. There are also four bands in the

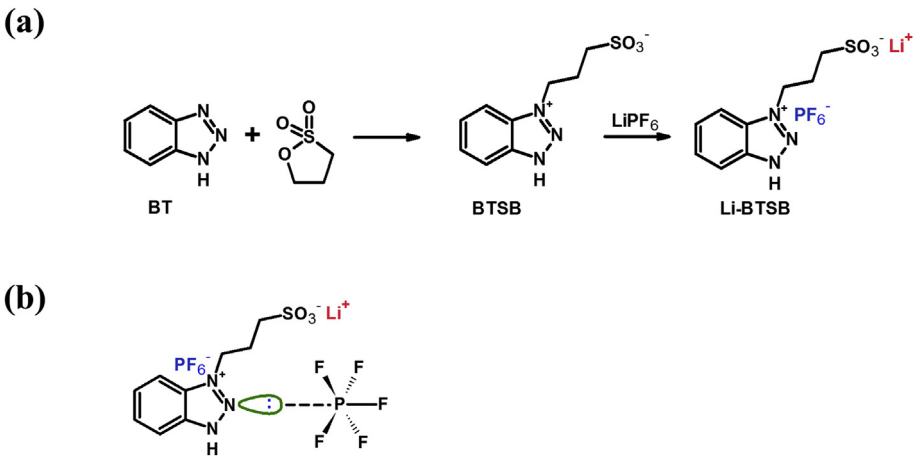

Scheme 1. (a) Synthesis and lithiation of the zwitterion benzotriazole-sulfobetaine (BTSB) to form the zwitterionic salt lithium-benzotriazole-sulfobetaine (Li-BTSB). (b) Splitting of $LiPF_6$ and dative bond formation with PF_5 into a complex in electrolyte by zwitterion.

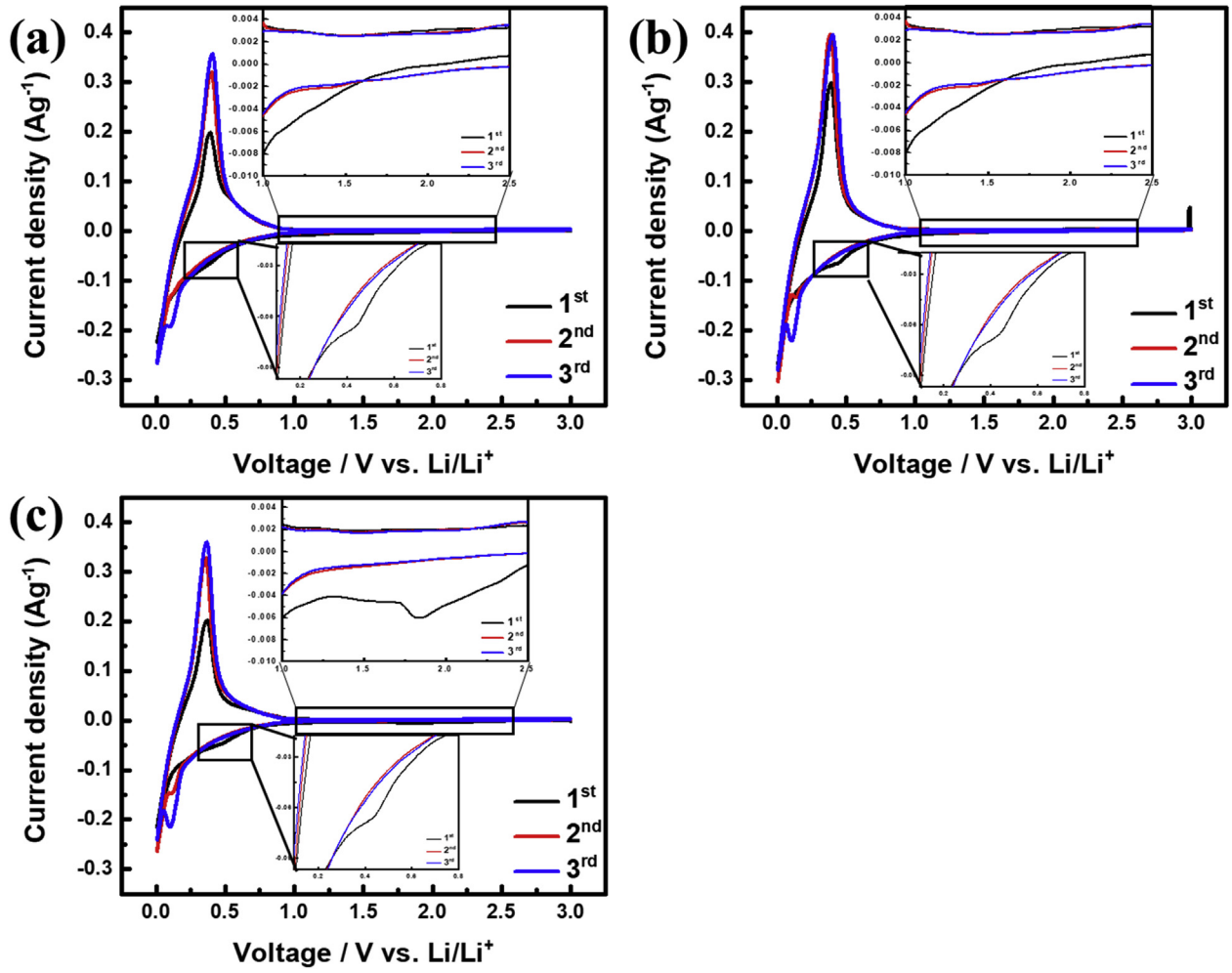

Fig. 3. Cyclic voltammograms of (a) pure electrolyte (b) 0.1 wt% BT and (c) 0.1 wt% Li-BTSB.

region 1612-1371 cm^{-1} due to C=C and C=N stretching vibrations. The spectrum of Li-BTSB shows a stretch at 1465 cm^{-1} is attributed to the C=N and N–H stretches in the quaternary ammonium group ($-N^{+}(CH_3)_2R-$). The peak at 1141 cm^{-1} is due to the symmetric and asymmetric stretching vibrations in the sulfonate group ($-SO_3^{-}$) on the zwitterion [42–45].

Fig. 1 (c) shows TGA curves for the BT and Li-BTSB from 100 to 800 °C done at 10 °C/min heating rate. The thermal decomposition (T_d) of the Li-BTSB is at around 268 °C compared to the T_d of BT, which is around 125 °C. A second thermal decomposition appeared around 322 °C for Li-BTSB and finished at around 489 °C. This behavior is the similar as the TGA trace of ionic liquids reported by Zhou et al. [46]. The higher T_d of the zwitterionic salt gives it an advantage over other molecular additives that are volatile [47].

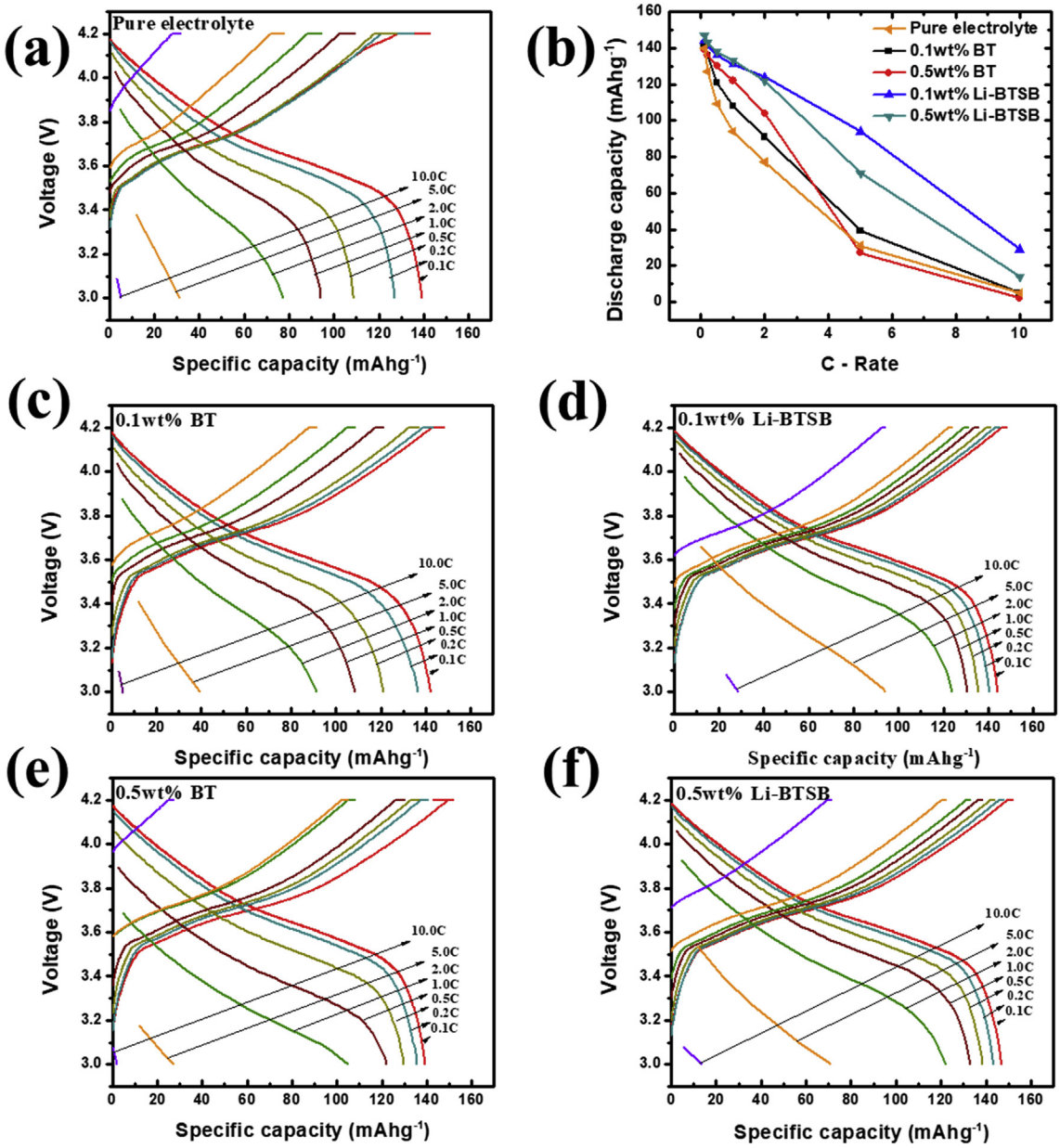

Fig. 4. Charge/discharge curves of (a) pure electrolyte, (b) discharge capacities as a function of C-rate of the, (c) 0.1 wt% BT, (d) 0.1 wt% Li-BTSB, (e) 0.5 wt% BT and (f) 0.5 wt% Li-BTSB electrolyte samples at a potential range of 3–4.2 V.

3.2. Electrochemical performance

3.2.1. Ionic conductivity

Fig. 2 (a) shows the Arrhenius plots of the ionic conductivities of the pure electrolyte, BT and Li-BTSB added electrolytes. Table 1 shows the summary of the ionic conductivities. In general, the temperature dependence of ionic conduction for electrolytes can be expressed by the Vogel–Fulcher–Tammann (VFT) equation (Equation (1)) [48], which explains the temperature dependence of viscosity in fluid materials.

$$\sigma = \sigma_0 \exp\left(\frac{-B}{T - T_0}\right) \quad (1)$$

where σ is the ionic conductivity, T is the temperature in Kelvin, and σ_0, B, and T_0 are constants. The plots show that the ionic conductivities exhibit the VFT behavior, which involves a decrease of ionic conductivity at low temperatures. The ionic conductivities shown in Table 1 were calculated from the Nyquist plot. The first value of the resistance acquired on the Z' axis was substituted into the conductivity equation given below.

$$C = \frac{l}{RA} \quad (2)$$

where R is the resistance on the Z' axis, A is the area of the electrode, and l is the separation of the electrodes. The electrolyte with BT has a slightly higher ionic conductivity compared to the pure electrolyte due to the Lewis-base nature of the base caused by the nitrogen atoms in the 5-member triazole ring, the $LiPF_6$ dissociation in the electrolyte is enhanced by forming weak dative bonds with the PF_5 (Scheme 1 b) [34]. However the Li-BTSB has the highest ionic conductivity because it has a quadruple effect i.e. (i) the Lewis-base nature of the benzotriazole base, (ii) the dipole moment of the zwitterion resulting in greater dissociation of the $LiPF_6$ salt due to immobilization of the PF_6^- anion on the N^+ of the zwitterion (Scheme 1) thus higher conductivity, (iii) The added Li^+ ions in the Li-BTSB increase Li^+ ion concentration in the electrolyte further enhancing the ionic conductivity [49,50] and (iv) It can also be stated that by formation of zwitterionic moieties on the BT, the ionic

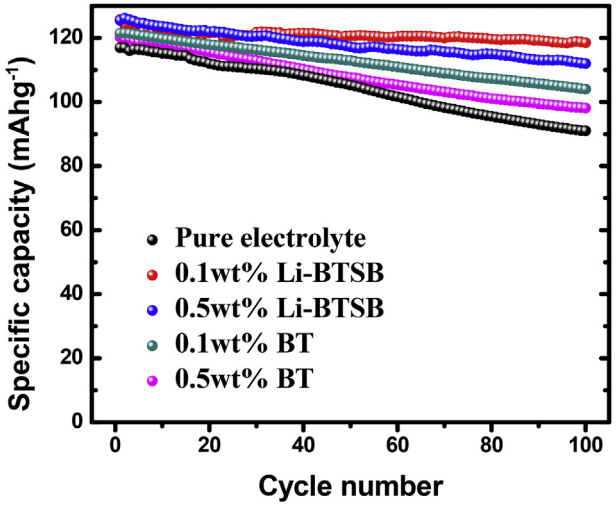

Fig. 5. Cycling performance of LCO/graphite cells adopting different electrolyte samples.

atmospheres will be eliminated by the competition of PF_6^- and SO_3^- moiety of the zwitterion towards the dissociated Li^+ ions resulting in easy migration of lithium ions hence increasing ionic conductivity [21,28–30]. Lithium ions are also immobilized on the SO_3^- group of the zwitterion hence it can be hypothesized that their movement is constrained. However, it has been reported that SO_3^- are good exchange sites for Li^+ ions because the SO_3^- group and Li^+ ions form a labile complex (easiness to associate and dissociate between the SO_3^- group and Li^+ ions), and therefore offer systematic ionic channels for movement of lithium ions [21,28–30]. However, concentrations of the zwitterion should be optimized because a continued increase of zwitterions results in a large number of SO_3^- anions encircled by Li^+ ions, which forms another ionic atmosphere that results in decreased ionic conductivity [51]. At low temperatures, the zwitterions self-assemble due to reduced mobility creating micro-channels that enhance Li^+ ion diffusion thereby enhancing ionic conductivity [3,4]. BT has also been used as an antifreeze [35] in aircraft de-icing fluids, because of this, it also enhances ionic conductivity at low temperature. The increase in ionic conductivity due to the addition of zwitterions to liquid EC-based electrolytes was also observed by Kim and co-workers when they added zwitterions containing an ether group to an electrolyte of $LiPF_6$ in a mixture of EC, DMC and EMC (1/1/1 v/v/v) [52] and also Krishna and coworkers who used imidazolium based zwitterions [53]. The Li-BTSB is also a bulky molecule due to the two rings of the BT base and therefore a higher concentration of the zwitterion will contribute to lower ionic conductivities [37] due to increased viscosity.

Table 2
Impedance characteristics after cell formation and 100 charge-discharge cycles.

Electrolyte	R_S	R_{SEI}	R_{ct}	R_W
(After cell formation)				
Pure electrolyte	4.788	12.795	22.095	0.202
0.1 wt% BT	2.627	6.947	21.188	0.147
0.5 wt% BT	2.661	8.685	17.719	0.152
0.1 wt% Li-BTSB	2.449	11.408	14.903	0.115
0.5 wt% Li-BTSB	2.527	11.658	15.138	0.121
(After 100 cycles)				
Pure electrolyte	5.163	17.614	31.655	0.318
0.1 wt% BT	4.391	7.947	32.179	0.315
0.5 wt% BT	4.645	9.887	20.939	0.294
0.1 wt% Li-BTSB	3.452	12.249	22.365	0.221
0.5 wt% Li-BTSB	3.658	12.339	22.549	0.239

Table 3
Elemental compositions of electrolytes[a].

	Atomic percentages (%)			
	C	O	F	P
Pure electrolyte	47.38	19.04	29.03	4.55
0.1 wt% BT	64.06	18.61	16.37	0.98
0.5 wt% BT	63.76	18.13	17.09	1.02
0.1 wt% Li-BTSB	69.07	15.92	14.12	0.91
0.5 wt% Li-BTSB	69.28	16.48	13.62	0.62

[a] Elemental compositions on graphite surfaces were determined after 100 cycles at 1.0 C-rate, using energy-dispersive X-ray spectroscopy.

3.2.2. Electrochemical stability

Fig. 2 (b) shows the LSVs of the different electrolyte samples. Electrolytes with a wide electrochemical window are essential for high voltage active materials. The pure electrolyte displays an anodic limit at ~4.6 V (vs. Li/Li^+). The electrolyte samples with BT and Li-BTSB display the anodic limit at ~5.5 V (vs. Li/Li^+) which shows that the electrochemical windows are greatly improved by adding either BT or Li-BTSB. This behavior is consistent with the electrochemical stability of imidazolium-based zwitterions, which exhibit an electrochemical window greater than 5 V [54–56]. The BT increases electrochemical stability due to its aromaticity and its corrosion-inhibition property enables it to reduce corrosion of the current collectors at higher voltages thereby increasing stability of the cell. The immobilization of the PF_6^- anions and the PF_5 by the Li-BTSB zwitterions and formation of an SEI on the surface of electrodes results in reduced contact between the PF_6^- anions and the electrode surface thereby reducing electrolyte decomposition [14,22,53,57].

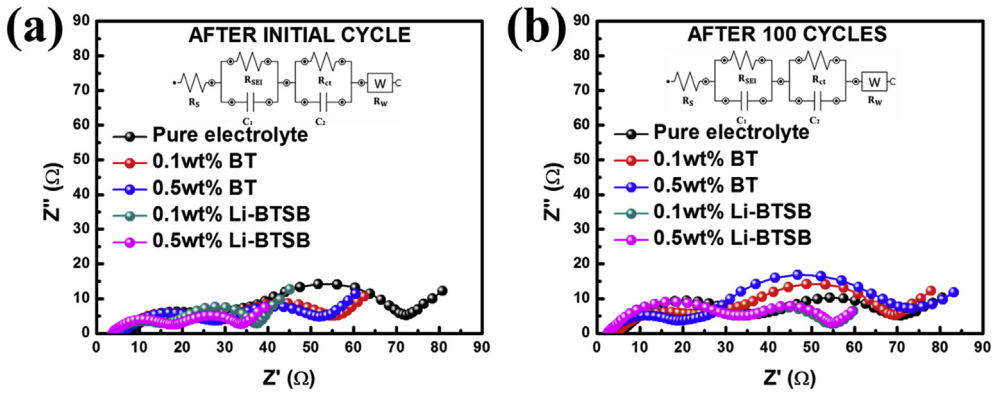

Fig. 6. Nyquist plots of LCO/graphite cells for electrolyte samples (a) after initial cycle and (b) after 100 cycles.

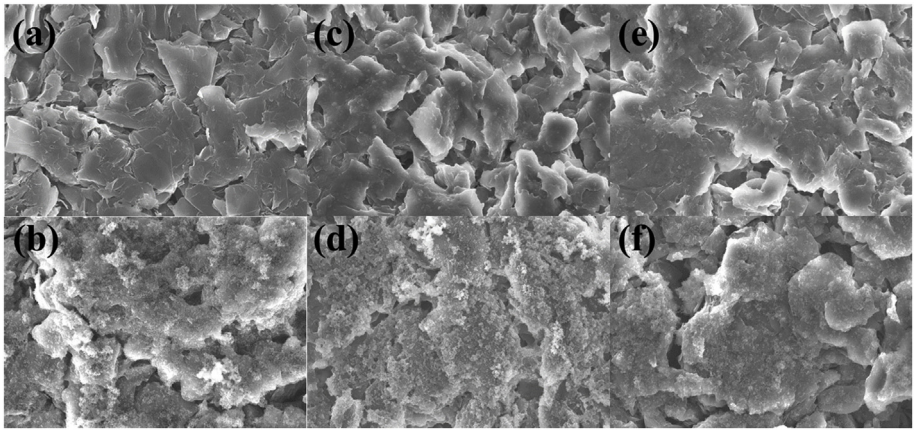

Fig. 7. Surface morphologies of the (a) unused graphite anode, and after 100 cycles for (b) pure electrolyte, (c) 0.1 wt% BT, (d) 0.1 wt% Li-BTSB, (e) 0.5 wt% BT and (f) 0.5 wt% Li-BTSB.

3.2.3. Cyclic voltammetry

CV measurements using graphite‖electrolyte‖Li cells were done in order to investigate the effect of zwitterions on the insertion of lithium ions into graphite. Fig. 3 shows the cyclic voltammograms for the cells containing pure electrolyte, 0.1 wt% BT and 0.1 wt% Li-BTSB electrolytes with graphite as the working electrode. For most EC-based electrolytes, an SEI is formed at potentials lower than 1 V vs. Li/Li^+ [58] hence an additive that forms an SEI at potentials higher than 1 V vs. Li/Li^+ reduces the decomposition of EC during SEI formation thereby protecting the electrolyte. Liquid additives are mostly used in organic electrolytes in order to enhance early and stable SEI formation on the graphite anode surface and to obviate exfoliation during the lithium intercalation. Vinylene carbonate (VC) is largely used because it has lower reductive activation energy and higher reduction potential (13 kcal/mol and 1.05–1.4 V Li/Li^+ respectively) compared to propylene carbonate (PC) (26.4 kcal/mol and 0.5–0.75 V Li/Li^+ respectively) and ethylene carbonate (EC) (24.9 kcal/mol and 0.65–0.9 V Li/Li+, respectively) [59–62]. The use of PC results in severe solvent co-intercalation with lithium ions into the graphite layers leading to their exfoliation, forming decomposition products within the graphite sheets and releasing gases like propylene [58]. On the other hand, EC has a high viscosity and melting point of 36 °C which necessitates the use of thinning solvents which lead to a highly flammable electrolyte [58]. Meanwhile, the use of VC in EC or PC increases the reduction potential by around 0.2 V making the solvent mixture to decompose earlier in the cell formation process compared to the without VC [62]. In our study, the cells with pure electrolyte, BT and Li-BTSB showed an irreversible peak from 0.54 V, 0.55 V and 1.25–1.76 V respectively, lithium intercalation cathodic peaks in the potential range of 0–0.2 V, and lithium deintercalation anodic peaks around 0.42 V vs. Li/Li^+. This shows that the zwitterionic Li-BTSB forms the passivating layer earlier before the decomposition of EC compared to the pure electrolyte and BT. During the 2nd and 3rd cycles, no current peak was observed near 0.54 V vs. Li/Li^+, which would be attributed to the decomposition of EC [37,63]. However, the electrolyte with BT had larger voltammograms than those with the pure electrolyte and Li-BTSB additive in the 1st cycle further proving that proving that lithium intercalation and deintercalation from the graphite was larger in the presence of BT. Therefore, it was concluded that BT was not involved in SEI formation [37].

3.2.4. Cell performances

Fig. 4 shows the charge/discharge profiles at different C-rates of the electrolyte samples with Fig. 4 (b) showing discharge capacity as a function of C-rate. It is apparent that the discharge capacity of the cell with each electrolyte is decreased with an increase in C-rate. The cells with the BT and Li-BTSB additives exhibited higher discharge capacities at higher C-rates compared to the pure electrolyte with the cells with the Li-BTSB additive displaying the highest discharge capacities. This improved performance is attributed to the higher ionic conductivities of the electrolytes with the Li-BTSB, electrolyte stability against oxidation on the graphite, improved stability of the $LiPF_6$ salt and the reduction of the SEI resistance thus allowing for efficient transport of lithium ions across the interface [64]. The cells with the Li-BTSB additive also had the least polarization with increasing C-rate hence higher discharge capacities at high C-rates [52]. There is also an increase in the difference between charge and discharge voltage plateaus as C-rate increases which explains that the cell is greatly restricted by Li^+ ion diffusion rate within the electrolyte and electrode/electrolyte interfaces [65]. Fig. 5 shows the cycling performance of the LCO/graphite cells using different electrolyte samples. In general, the discharge capacity of $LiCoO_2$ declines at cut-off voltages > 4.3 V in the absence of metal oxide surface coatings such as ZrO_2, Al_2O_3 and Li_2CO_3 on the $LiCoO_2$ which can be due to reasons such as the structural change of the dissolution of Co ions and $LiCoO_2$ [66]. The electrolyte with Li-BTSB (0.1 wt% showing the best cycling performance) showed the best cycling performance with a high capacity retention of 94% compared to the pure electrolyte with the lowest capacity retention of 78%. This shows the effectiveness of Li-BTSB as an additive in lowering the rate of capacity fading in LCO cells at a high cut-off voltage.

An additive should also be able to form a stable and moderate SEI layer for it to be effective in LIBs [67], which is analyzed using electrochemical impedance spectroscopy (EIS). Nyquist plots obtained from EIS allow us to determine resistances from two consecutive semicircles proceeded by a diagonal line. The intercept in the real axis gives the bulk or solution resistance (R_s), the diameter of the small semicircle in the high-frequency range gives the interfacial or SEI resistance (R_{SEI}) [68]. The diameter of the big semicircle in the intermediate-frequency range gives the Charge transfer resistance (R_{ct}) in the electrodes, and the Warburg impedance (R_W) at the low-frequency range describes the lithium-ion diffusion into the graphite electrode [67]. Nyquist plots for the LCO/graphite cells are shown in Fig. 6 and corresponding values are summarized in Table 2. It should be noted that almost all the SEI contribution in this case is due to the SEI on the graphite surface because the SEI mostly forms on the graphite electrode due to electrolyte decomposition (although the SEI forms on the cathode, it is considered negligible) [69,70]. The R_s increases from the 1st cycle to the 100th cycle as expected due to electrolyte decomposition. From Fig. 6 and Table 2, it is observed that the R_s for the pure electrolyte is higher compared to the other electrolytes. Considering the components of the SEI (Table 3), the electrolytes with BT had the smallest R_{SEI} than those the pure electrolyte and Li-BTSB. This is because BT is not directly involved in the formation of the SEI, but rather improves the SEI stability

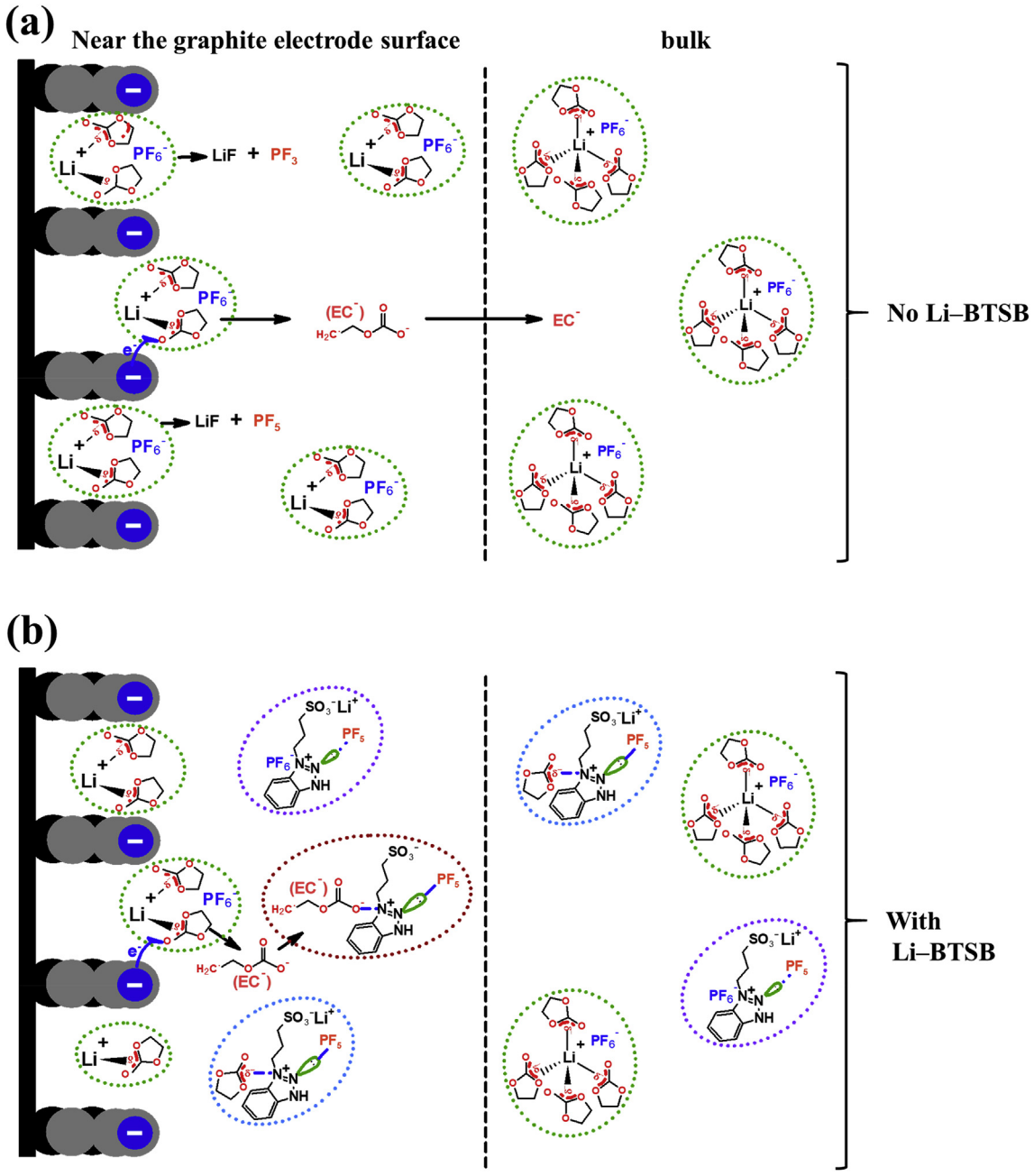

Fig. 8. Postulate of behaviour of electrolyte molecules in (a) pure electrolyte (1 M $LiPF_6$ in EC:DMC 1:1) (b) pure electrolyte + 0.1 wt% Li-BTSB.

due to its ability to stabilize the $LiPF_6$ salt against further decomposition due to the ability of BT to couple with PF_6^- in the electrolyte and also formation of dative bonds with PF_5 consequently suppressing side reactions [34,37]. The Li-BTSB has a smaller R_{SEI} than pure electrolyte because the zwitterionic Li-BTSB enable the formation of SEI film on the surface of graphite electrode and they can immobilize the PF_6^- anions (Scheme 1 b). This limits contact between the PF_6^- anions and the graphite electrode hence a lower concentration of PF_6^- anions on the cathode resulting in reduced electrolyte degradation [17,53,70]. Its known that EC may undergo a ring-opening reaction to form a stable radical anion (EC^-) (Fig. 7) [60] which is either reduced to form carbonate (CO_3^{2-}) and ethylene (C_2H_2) or react with another EC^- to form ethylene dicarbonate (EDC^{2-}) close to the electrode [71]. Although the SEI structure varies with the solvent mixture ratio of EC:DMC [72], it has been suggested that the formation of EDC^{2-} is highly probable in systems with relatively high EC concentrations, like 1:1 EC:DMC due to the high possibility of EC^- combination [73]. This would lead to more decomposition of the electrolyte solvent and consequently, the formation of a thicker and more diffuse SEI layer [71]. As observed, electrolytes with the Li-BTSB additive show smaller R_{SEI}, thus we hypothesize that (i) movement of the EC^- into the bulk solution is suppressed by the zwitterion molecules near the electrode surface due to the immobilizing of EC^- molecules on the N^+ (Fig. 7). (ii) Moreover, the zwitterions and the EC molecules in the bulk form intermolecular interactions with each other hence the movement of EC molecules towards the electrodes is decreased in so doing reducing further decomposition of the electrolyte resulting in a more stable SEI.

The surface morphologies of the graphite electrodes after cell formation are shown in Fig. 8. From the SEM images, it can be observed that SEI film is formed and spread across the surface of the electrode. The elemental analysis using EDX is summarized in Table 3. The lower F and P in the SEI formed with electrolytes with Li-BTSB compared to

those with the pure electrolyte shows that the zwitterion forms a more stable SEI and are more effective in preventing electrolyte decomposition [64]. The reduction and decomposition of PF_6^- directly generates PF_5 and F^-, which would form LiF with Li^+ which occurs before the reduction of EC [74] as shown in Equations (3) and (4).

$$PF_6^- + 3Li^+ + 2e^- \rightarrow 3LiF \downarrow + PF_3\uparrow \quad (3)$$

$$LiPF_6 \rightarrow LiF \downarrow + PF_5\uparrow \quad (4)$$

Greater decomposition of the $LiPF_6$ electrolyte salt results in a higher percentage of fluorine and phosphorus in the SEI. Zwitterionic salt Li-BTSB could have impeded the decomposition reactions (Equations (3) and (4)) of $LiPF_6$ resulting in a lower percentage of phosphorus and fluorine. We theorize that the zwitterions may have been able to do this by interfering with the Li^+ solvation sheath that consists of a Li^+ ion tetrahedrally solvated by four EC molecules in the primary solvation shell and an PF_6^- anion in the close but outside of the primary sheath (Fig. 7). As the solvated Li^+ ion approaches the graphite edge, the graphite expands under a strain and the solvated Li^+ loses two EC molecules to minimize the co-intercalation energy barrier (Fig. 7) [75–77]. The EC is stripped first in the process because the solvation energy of EC is smaller than that of PF_6^-, resulting in a partially desolvated Li^+ containing PF_6^- that will co–intercalate into the graphite thus becoming precursors for final SEI through reductive decomposition [75]. The PF_6^- ions can undergo reductive decomposition when complexed with Li^+ ions because it is thermodynamically improbable for a lone PF_6^- to gain an electron since the reductive activity of PF_6^- is lower than that of EC [75]. The PF_6^- ion are immobilized by the zwitterion thus isolating them and in the process distorting the solvation sheath and also reducing the number of PF_6^- that are co–intercalated into the graphite. This we postulate that it subdues the reductive decomposition of PF_6^- ions. These postulates would need to be investigated by computational modelling.

All these phenomena help in the formation of a stable SEI and reduce the decomposition of the electrolyte at high voltages in cells with electrolytes containing the Li-BTSB additive. A stable SEI layer allows easy conduction of lithium ions resulting in better cycling performance. The lower R_{SEI} and R_W values and the high ionic conductivities as well as an electrochemical stability displayed by the electrolytes with the Li-BTSB additive are the major results of this study.

4. Conclusion

Zwitterionic Li-BTSB was synthesized and used as a liquid electrolyte additive for LIBs. Electrolyte samples with the Li-BTSB additive dissolved in 1 M $LiPF_6$ (EC/DMC = 1:1) showed a high ionic conductivity and an excellent electrochemical stability. The LCO/graphite cells with the electrolyte samples with the Li-BTSB showed greater discharge capacities at higher C-rates due to increased ionic conductivity. The LCO/graphite cells also showed stable cycling performance. The high performance electrolyte additive can greatly increase energy density due to its high voltage window and increase power density due to its high ionic conductivity. The Li-BTSB additive is therefore a strong candidate for use as a liquid electrolyte additive for high voltage LIB batteries.

Declaration of competing interest

The authors declare that they have no known competing financial interests or personal relationships that could have appeared to influence the work reported in this paper.

Acknowledgements

This research was supported by the research fund of Hanbat National University in 2019.

References

[1] S. Yang, Y. Gong, Z. Liu, L. Zhan, D.P. Hashim, L. Ma, R. Vajtai, P.M. Ajayan, Bottom-up approach toward single-crystalline VO_2-graphene ribbons as cathodes for ultrafast lithium storage, Nano Lett. 13 (2013) 1596–1601.
[2] B. Ji, F. Zhang, M. Sheng, X. Tong, Y. Tang, A novel and generalized lithium-ion-battery configuration utilizing Al foil as both anode and current collector for enhanced energy density, Adv. Mater. 29 (1–7) (2017).
[3] G. Ma, S. Li, W. Zhang, Z. Yang, S. Liu, X. Fan, F. Chen, Y. Tian, W. Zhang, S. Yang, M. Li, A general and mild approach to controllable preparation of manganese-based micro- and nanostructured bars for high performance lithium-ion batteries, Angew. Chem. Int. Ed.Energy Storage Mater. 55 (2016) 3667–3671.
[4] S.S. Zhang, A review on the separators of liquid electrolyte Li-ion batteries, J. Power Sources 164 (2007) 351–364.
[5] J. Sun, P. Bayley, D.R. Macfarlane, M. Forsyth, Gel electrolytes based on lithium modified silica nanoparticles, Electrochim. Acta 52 (2007) 7083–7090.
[6] L. Yue, J. Ma, J. Zhang, J. Zhao, S. Dong, Z. Liu, G. Cui, L. Chen, All solid-state polymer electrolytes for high-performance lithium ion batteries, Energy Storage Mater. 5 (2016) 139–164.
[7] W. Zhao, Y. Ji, Z. Zhang, M. Lin, Z. Wu, X. Zheng, Q. Li, Y. Yang, Recent advances in the research of functional electrolyte additives for lithium-ion batteries, Curr. Opin. Electrochem. 6 (84–91) (2017).
[8] D.Y. Park, D.Y. Park, Yu-Lan, Y.S. Lim, M.S. Kim, High rate capability of carbonaceous composites as anode electrodes for lithium-ion secondary battery, J. Ind. Eng. Chem. 15 (2009) 588–594.
[9] M. Dahbi, F. Ghamouss, F. Tran-Van, D. Lemordant, M. Anouti, Comparative study of EC/DMC LiTFSI and $LiPF_6$ electrolytes for electrochemical storage, J. Power Sources 196 (2011) 9743–9750.
[10] V. Aravindan, J. Gnanaraj, S. Madhavi, H.K. Liu, Lithium-ion conducting electrolyte salts for lithium batteries, Chem. Eur J. 17 (2011) 14326–14346.
[11] H. Wang, M. Yoshio, A.K. Thapa, H. Nakamura, From symmetric AC/AC to asymmetric AC/graphite, a progress in electrochemical capacitors, J. Power Sources 169 (2007) 375–380.
[12] D. Aurbach, Y. Talyosef, B. Markovsky, E. Markevich, E. Zinigrad, L. Asraf, J.S. Gnanaraj, H.J. Kim, Design of electrolyte solutions for Li and Li-ion batteries: a review, Electrochim. Acta 50 (2004) 247–254.
[13] A.R. Polu, H.W. Rhee, M. Jeevan Kumar Reddy, A.M. Shanmugharaj, S.H. Ryu, D.K. Kim, Effect of POSS-PEG hybrid nanoparticles on cycling performance of polyether-LiDFOB based solid polymer electrolytes for all solid-state Li-ion battery applications, J. Ind. Eng. Chem. 45 (2017) 68–77.
[14] J. Ha, S. Im, S. Lee, H. Jang, T. Ryu, C. Lee, Y. Jeon, W. Kim, Liquid type of fluorosulfonyl lithium salts containing siloxane for Li-ion electrolyte, J. Ind. Eng. Chem. 37 (2016) 319–324.
[15] J.S. Gnanaraj, M.D. Levi, Y. Gofer, D. Aurbach, M. Schmidt, LiPF[sub3] (CF [sub2] CF[sub 3])[sub 3]: a salt for rechargeable lithium ion batteries, J. Electrochem. Soc. 150 (2003) A445.
[16] F. Kita, H. Sakata, S. Sinomoto, A. Kawakami, H. Kamizori, T. Sonoda, H. Nagashima, J. Nie, N.V. Pavlenko, Y.L. Yagupolski, Characteristics of the electrolyte with fluoro organic lithium salts, J. Power Sources 90 (2000) 27–32.
[17] S. Yamaguchi, M. Yoshizawa-fujita, H. Zhu, M. Forsyth, Y. Takeoka, M. Rikukawa, Improvement of charge/discharge properties of oligoether electrolytes by zwitterions with an attached cyano group for use in lithium-ion secondary batteries, Electrochim. Acta 186 (2015) 471–477.
[18] F. Wohde, R. Bhandary, J.M. Moldrickx, J. Sundermeyer, M. Schönhoff, B. Roling, Li^+ ion transport in ionic liquid-based electrolytes and the influence of sulfonate-based zwitterion additives, Solid State Ion. 284 (2016) 37–44.
[19] Q. Shao, L. Mi, X. Han, T. Bai, S. Liu, Y. Li, S. Jiang, Differences in cationic and anionic charge densities dictate zwitterionic associations and stimuli responses, J. Phys. Chem. B 118 (2014) 6956–6962.
[20] F. Lind, L. Rebollar, P. Bengani-Lutz, A. Asatekin, M.J. Panzer, Zwitterion-containing ionogel electrolytes, Chem. Mater. 28 (2016) 8480–8483.
[21] C. Tiyapiboonchaiya, J.M. Pringle, J. Sun, N. Byrne, P.C. Howlett, D.R. Macfarlane, M. Forsyth, The zwitterion effect in high-conductivity polyelectrolyte materials, Nat. Mater. 3 (29–32) (2004).
[22] Q. Shao, Y. He, S. Jiang, Molecular dynamics simulation study of ion interactions with zwitterions, J. Phys. Chem. B 115 (2011) 8358–8363.
[23] M. Yoshizawa, A. Narita, H. Ohno, Design of ionic liquids for electrochemical applications, Aust. J. Chem. 57 (2004) 139–144.
[24] H. Lee, D.B. Kim, S.H. Kim, H.S. Kim, S.J. Kim, D.K. Choi, Y.S. Kang, J. Won, Zwitterionic silver complexes as carriers for facilitated-transport composite membranes, Angew. Chem. Int. Ed. 43 (2004) 3053–3056.
[25] H. Ohno, M. Yoshizawa, W. Ogihara, A new type of polymer gel electrolyte: zwitterionic liquid/polar polymer mixture, Electrochim. Acta 48 (2003) 2079–2083.
[26] M. Yoshizawa, M. Hirao, K. Ito-Akita, H. Ohno, Ion conduction in zwitterionic-type molten salts and their polymers, J. Mater. Chem. 11 (2001) 1057–1062.
[27] M. Yoshizawa-Fujita, N. Byrne, M. Forsyth, D.R. MacFarlane, H. Ohno, Proton transport properties in zwitterion blends with Brønsted acids, J. Phys. Chem. B 114 (2010) 16373–16380.
[28] K. Ito, N. Nishina, H. Ohno, High lithium ionic conductivity of poly(ethylene oxide) s having sulfonate groups on their chain ends, J. Mater. Chem. 7 (1997) 1357–1362.
[29] A. Narita, W. Shibayama, H. Ohno, Structural factors to improve physico-chemical properties of zwitterions as ion conductive matrices, J. Mater. Chem. 16 (2006) 1475–1482.
[30] R. Rondla, J.C.Y. Lin, C.T. Yang, I.J.B. Lin, Strong tendency of homeotropic alignment and anisotropic lithium ion conductivity of sulfonate functionalized

zwitterionic imidazolium ionic liquid crystals, Langmuir 29 (2013) 11779–11785.
[31] N. Byrne, P.C. Howlett, D.R. MacFarlane, M.E. Smith, A. Howes, A.F. Hollenkamp, T. Bastow, P. Hale, M. Forsyth, Effect of zwitterion on the lithium solid electrolyte interphase in ionic liquid electrolytes, J. Power Sources 184 (2008) 288–296.
[32] B.N. Byrne, P.C. Howlett, D.R. Macfarlane, M. Forsyth, The zwitterion effect in ionic Liquids : towards practical rechargeable lithium-metal batteries, Adv. Mater. 17 (2005) 2497–2501.
[33] A. Abouimrane, I.J. Davidson, Solid electrolyte based on succinonitrile and LiBOB, J. Electrochem. Soc. 154 (2007) A1031–A1034.
[34] S.A. Pradanawati, F.M. Wang, J. Rick, In Situ formation of pentafluorophosphate benzimidazole anion stabilizes high-temperature performance of lithium-ion batteries, Electrochim. Acta 135 (2014) 388–395.
[35] E. Abdullayev, R. Price, D. Shchukin, Y. Lvov, Halloysite tubes as nanocontainers for anticorrosion coating with benzotriazole, ACS Appl. Mater. Interfaces 1 (2009) 1437–1443.
[36] R. Ravichandran, S. Nanjundan, N. Rajendran, Effect of benzotriazole derivatives on the corrosion of brass in NaCl solutions, Appl. Surf. Sci. 236 (2004) 241–250.
[37] L. Hamenu, Alfred Madzvamuse, Latifatu Mohammed, Yong min lee, Jang myoun Ko, chris Yeajoon bon, sang Jun Kim, Won il cho, Yong gu baek, Jongwook park, benzotriazole as an electrolyte additive on lithium-ion batteries performance, J. Ind. Eng. Chem. 53 (2017) 241–246.
[38] L.Z. Fan, Y.S. Hu, A.J. Bhattacharyya, J. Maier, Succinonitrile as a versatile additive for polymer electrolytes, Adv. Funct. Mater. 17 (2007) 2800–2807.
[39] J.F. Moulder, W.F. Stickle, P.E. Sobol, K.D. Bomben, Handbook of X-Ray Photoelectron Spectroscopy, Perkin-Elmer, Boca Raton, FL, 1992.
[40] S.H. Ye, C.A. Johnson Jr., J.R. Woolley, H. Murata, L.J. Gamble, K. Ishihara, W.R. Wagner, Simple surface modification of a titanium alloy with silanated zwitterionic phosphorylcholine or sulfobetaine modifiers to reduce thrombogenicity, Colloids Surfaces B Biointerfaces 79 (2010) 357–364.
[41] S. Yeh, C. Chen, W. Chen, C. Huang, Modification of silicone Elastomer with zwitterionic silane for durable Antifouling properties, Langmuir 30 (2014) 11386–11393.
[42] G. Socrates, Infrared Characteristic Group Frequencies, John Wiley & Sons, Bristol, 2001.
[43] Y. Song, Y. Sun, X. Zhang, J. Zhou, L. Zhang, Homogeneous quaternization of cellulose in NaOH/Urea Aqueous solutions as gene carriers, Biomacromolecules 9 (2008) 2259–2264.
[44] B.R. Knowles, P. Wagner, S. McLaughlin, M.J. Higgins, P.J. Molino, Silica nanoparticles functionalized with zwitterionic sulfobetaine siloxane for Application as a versatile Antifouling coating system, ACS Appl. Mater. Interfaces 9 (2017) 18584–18594.
[45] L.S. Barreto, M.S. Tokumoto, I.C. Guedes, H.G. de Melo, F.D. Rico Amado, V.R. Capelossi, Evaluation of the anticorrosion performance of peel garlic extract as corrosion inhibitor for ASTM 1020 carbon steel in acidic solution, Rev. Mater. 22 (2017).
[46] Q. Zhou, W.A. Henderson, G.B. Appetecchi, S. Passerini, Phase behavior and thermal properties of ternary ionic liquid - lithium salt (IL - IL - LiX) electrolytes, J. Phys. Chem. C 114 (2010) 6201–6204.
[47] N. Wongittharom, C.H. Wang, Y.C. Wang, G.T.K. Fey, H.Y. Li, T.Y. Wu, T.C. Lee, J.K. Chang, Charge-storage performance of Li/$LiFePO_4$ cells with additive incorporated ionic liquid electrolytes at various temperatures, J. Power Sources 260 (2014) 268–275.
[48] M.G. McLin, C.A. Angell, Ion-pairing effects on viscosity/conductance relations in Raman-characterized polymer electrolytes: lithium perchlorate and sodium triflate in PPG(4000), J. Phys. Chem. 95 (1991) 9464–9469.
[49] J. Sun, D.R. Macfarlane, N. Byrne, M. Forsyth, Zwitterion effect in polyelectrolyte gels based on lithium methacrylate- N , N -dimethyl acrylamide copolymer, Electrochim. Acta 51 (2006) 4033–4038.
[50] M. Latifatu, M. Hu, S. Jun, C. Yeajoon, C. Kang, W.I. Cho, J.M. Ko, Lithium modified silica as electrolyte additive for lithium secondary batteries, Solid State Ion. 319 (7–12) (2018).
[51] M. Suematsu, M. Yoshizawa-fujita, H. Zhu, M. Forsyth, Y. Takeoka, M. Rikukawa, Effect of zwitterions on electrochemical properties of oligoether-based electrolytes Endothermic G5/LiFSA Temperature/°C, Electrochim. Acta 175 (2015) 209–213.
[52] H. Kim, D.Q. Nguyen, H.W. Bae, J.S. Lee, B.W. Cho, H.S. Kim, M. Cheong, H. Lee, Effect of ether group on the electrochemical stability of zwitterionic imidazolium compounds, Electrochem. Commun. 10 (2008) 1761–1764.
[53] J.N. Krishnan, H.S. Kim, J.K. Lee, B. Cho, E.J. Roh, S. Lee, Organic solvents containing zwitterion as electrolyte for Li ion cells, Bull. Korean Chem. Soc. 29 (2010) 1705–1710.
[54] N. Sun, X. Gao, A. Wu, F. Lu, L. Zheng, Mechanically strong ionogels formed by immobilizing ionic liquid in polyzwitterion networks, J. Mol. Liq. 248 (2017) 759–766.
[55] P. Bengani-Lutz, E. Converse, P. Cebe, A. Asatekin, Self-assembling zwitterionic copolymers as membrane selective layers with excellent fouling resistance: effect of zwitterion chemistry, ACS Appl. Mater. Interfaces 9 (2017) 20859–20872.
[56] M. Suematsu, M. Yoshizawa-Fujita, T. Tamura, Y. Takeoka, M. Rikukawa, Dependence of transport properties of concentrated lithium salt solutions on temperature and composition in an imidazolium-based liquid zwitterion containing an oligo(ethylene oxide) unit, Int. J. Electrochem. Sci. 10 (2015) 248–258.
[57] D.Q. Nguyen, H.W. Bae, E.H. Jeon, J.S. Lee, M. Cheong, H. Kim, H.S. Kima, H. Lee, Zwitterionic imidazolium compounds with high cathodic stability as additives for lithium battery electrolytes, J. Power Sources 183 (2008) 303–309.
[58] S.J. An, J. Li, C. Daniel, D. Mohanty, S. Nagpure, D.L. Wood, The state of understanding of the lithium-ion-battery graphite solid electrolyte interphase (SEI) and its relationship to formation cycling, Carbon N. Y. 105 (2016) 52–76.
[59] V. Etacheri, R. Marom, R. Elazari, G. Salitra, D. Aurbach, Challenges in the development of advanced Li-ion batteries: a review, Energy Environ. Sci. 4 (2011) 3243–3262.
[60] K. Tasaki, K. Kanda, T. Kobayashi, S. Nakamura, M. Ue, Theoretical studies on the reductive decompositions of solvents and additives for lithium-ion batteries near lithium anodes, J. Electrochem. Soc. 153 (2006) A2192.
[61] S. Flandrois, B. Simon, Carbon materials for lithium-ion rechargeable batteries, Carbon N. Y. 37 (1999) 165–180.
[62] S.H. Lee, H.G. You, K.S. Han, J. Kim, I.H. Jung, J.H. Song, A new approach to surface properties of solid electrolyte interphase on a graphite negative electrode, J. *Power Sources* 247 (2014) 307–313.
[63] P. Novák, F. Joho, R. Imhof, J.C. Panitz, O. Haas, In situ investigation of the interaction between graphite and electrolyte solutions, J. Power Sources 81–82 (1999) 212–216.
[64] L. Hamenu, H.S. Lee, M. Latifatu, K.M. Kim, J.W. Park, Y.G. Baek, J.M. Ko, R.B. Kaneret, Lithium-silica nanosalt as a low-temperature electrolyte additive for lithium-ion batteries, Curr. Appl. Phys. 16 (2016) 611–617.
[65] M. Liu, B. Jin, Q. Zhang, X. Zhan, F. Chen, High-performance solid polymer electrolytes for lithium ion batteries based on sulfobetaine zwitterion and poly (ethylene oxide) modified polysiloxane, J. Alloy. Comp. 742 (2018) 619–628.
[66] C. Li, H.P. Zhang, L.J. Fu, H. Liu, Y.P. Wu, E. Rahm, R. Holze, H.Q. Wu, Cathode materials modified by surface coating for lithium ion batteries, Electrochim. Acta 51 (2006) 3872–3883.
[67] I.A. Profatilova, S.S. Kim, N.S. Choi, Enhanced thermal properties of the solid electrolyte interphase formed on graphite in an electrolyte with fluoroethylene carbonate, Electrochim. Acta 54 (2009) 4445–4450.
[68] X. Zuo, C. Fan, X. Xiao, J. Liu, J. Nan, High-voltage performance of $LiCoO_2$/graphite batteries with methylene methanedisulfonate as electrolyte additive, J. Power Sources 219 (2012) 94–99.
[69] M. Itagaki, N. Kobari, S. Yotsuda, K. Watanabe, S. Kinoshita, M. Ue, $LiCoO_2$ electrode/electrolyte interface of Li-ion rechargeable batteries investigated by in situ electrochemical impedance spectroscopy, J. Power Sources 148 (2005) 78–84.
[70] P. Verma, P. Maire, P. Novák, A review of the features and analyses of the solid electrolyte interphase in Li-ion batteries, Electrochim. Acta 55 (2010) 6332–6341.
[71] M.J. Boyer, G.S. Hwang, Theoretical evaluation of ethylene carbonate anion transport and its impact on solid electrolyte interphase formation, Electrochim. Acta 266 (2018) 326–331.
[72] D. Aurbach, A comparative study of synthetic graphite and Li electrodes in electrolyte solutions based on ethylene carbonate-dimethyl carbonate mixtures, J. Electrochem. Soc. 143 (1996) 3809.
[73] D. Aurbach, B. Markovsky, I. Weissman, E. Levi, Y. Ein-eli, On the correlation between surface chemistry and performance of graphite negative electrodes for Li ion batteries, Electrochim. Acta 45 (67 – 86) (1999).
[74] T. Kawaguchi, K. Shimada, T. Ichitsubo, S. Yagi, E. Matsubara, Surface-layer formation by reductive decomposition of LiPF6 at relatively high potentials on negative electrodes in lithium ion batteries and its suppression, J. *Power Sources* 271 (2014) 431–436.
[75] J.O. Besenhard, M. Winter, J. Yang, W. Biberacher, Filming mechanism of lithium-carbon anodes in organic and inorganic electrolytes, J. Power Sources 54 (1995) 228–231.
[76] L. Xing, X. Zheng, M. Schroeder, J. Alvarado, A. von Wald Cresce, K. Xu, Q. Li, W. Li, Deciphering the ethylene carbonate-propylene carbonate mystery in Li-ion batteries, Acc. Chem. Res. 51 (2018) 282–289.
[77] M. R Wagner, J.H. Albering, K.C. Moeller, J.O. Besenhard, M. Winter, XRD Evidence for the electrochemical formation of in PC-based electrolytes, Electrochem. Commun. 7 (2005) 947–952.